FED-Vol. 246/MD-Vol. 81, Rheology and Fluid Mechanics
of Nonlinear Materials — 1998
ASME 1998

FLOW PATTERNS OF VISCOELASTIC FLUIDS IN A PLANAR CONTRACTION OBTAINED WITH A FINITE-VOLUME SIMULATION

Paulo J. Oliveira[1]
Departamento de Engenharia Electromecânica
Universidade da Beira Interior
Rua Marquês D'Ávila e Bolama
6200 Covilhã, Portugal
pjpo@ubi.pt

Fernando T. Pinho[1]
Departamento de Engenharia Mecânica
e Gestão Industrial
Faculdade de Engenharia, Universidade do Porto
Rua dos Bragas, 4099 Porto Codex, Portugal
fpinho@fe.up.pt

ABSTRACT

A new general finite-volume method based on an efficient collocated mesh arrangement, with the added advantage of indirect addressing, has been applied to predict the flow of UCM fluids in a 4:1 sudden planar contraction. First and second order differencing schemes were used, and the Deborah number ranged from 0 to 10 for a Reynolds number of 0.01.

The predicted flow patterns showed all the flow features seen in flow visualisation and in recent numerical simulations of contraction flows, namely the corner Moffat vortex, the lip vortex, the fingering and merging of the two vortex types and single vortex growth with Deborah number. The presence of a lip vortex is detected at a Deborah number of 2 and the observations of those flow features requires very fine meshes in the vicinity of the contraction plane.

KEYWORDS: finite-volume, lip vortex, Upper Convected Maxwell model, contraction flow

1. INTRODUCTION

Viscoelastic flows through sudden contractions, both in planar and round configurations, have received quite a lot of attention in the past couple of decades because they offer a relatively simple geometry adequate for numerical simulations, and also because they are related to some practical applications, such as extrusion processes.

In spite of the simple geometry, contraction flows of viscoelastic fluids pose severe numerical problems because the re-entrant corner represents a singularity near which the stress components tend to infinity. Furthermore, as observed by Boger et al (1986) and Evans and Walters (1986), the flow patterns are rather more complex than anticipated. The recirculating corner vortex tends to increase in size and intensity with the elasticity of the fluid, as measured by the Deborah or Weissenberg numbers, but in certain circunstances there is also a lip vortex appearing in the re-entrant corner, which interacts and eventually merges with the former corner vortex, as De is increased.

These features, specifically the occurence of the lip vortex, have been observed in experimental investigations but could not be obtained with numerical simulations when the constitutive models used to represent the characteristics of the fluid were of the Maxwell or Oldroyd-B type. In some instances a small sporadic lip vortex would be predicted, but the authors themselves would consider it as a numerical artifact due to poor mesh resolution (Marchal and Crochet, 1987) or to some transient feature (Sato and Richardson, 1994). For example, Marchal and Crochet (1987) in the well-known paper on the streamline-upwind scheme for finite-element method, used the contraction flow of an Oldroyd-B fluid as a test case and clearly stated that the planar flow was unchanged from the Newtonian case, even at high elasticity, being a particularly un-interesting flow example. This state of things induced, at the time, some discredit into the foreseen possibilities of numerical simulations to represent the complexities observed in real flows (see, for example, Boger's review (1987) and Evans and Walters, 1986).

The purpose of this paper is to show that the lip vortex and its interaction with the main corner vortex, features oberved in the experiments, can be numerically simulated with an upper-convected Maxwell fluid, provided the mesh used in the computations is sufficiently fine to resolve well the flow features. To this aim, a general finite-volume method recently developed by the authors is applied to the two-dimensional problem of viscoelastic flow through a 4-to-1 abrupt contraction. Systematic mesh refinement is carried out to ensure that the solution is convergent (except in the near vicinity of the singularity) and to emphasize the differences arising in the flow patterns purely due to insufficient mesh resolution.

[1] correspondence can be sent to either author

2. GOVERNING EQUATIONS

The basic equations are those for three-dimensional, incompressible and isothermal laminar flow of an upper convected Maxwell model fluid, hereafter referred to as the UCM fluid. Unless otherwise stated or for outlined indices, the summation convention for repeated indices will apply to either Cartesian components (*i, j,* ...) or non-Cartesian (*l, m,* ...) directions.

The continuity equation is

$$\frac{\partial u_i}{\partial x_i} = 0 \tag{1}$$

and the momentum conservation equation is given by

$$\frac{\partial \rho u_i}{\partial t} + \frac{\partial}{\partial x_j}\left(\rho u_i u_j\right) = -\frac{\partial p}{\partial x_i} + \frac{\partial \tau_{ij}}{\partial x_j} + \rho g_i \tag{2}$$

where the extra stress tensor τ_{ij} is defined by the UCM constitutive equation

$$\tau_{ij} + \lambda \tau_{(1)ij} = \eta\left[\frac{\partial u_i}{\partial x_j} + \frac{\partial u_j}{\partial x_i}\right] - \frac{2}{3}\eta \frac{\partial u_k}{\partial x_k}\delta_{ij} \tag{3}$$

The last term on the right-hand-side (rhs) of the constitutive equation is zero for incompressible fluids, such as those analysed here, but it is kept because it is not exactly zero in the numerical approximation and improves the convergence rate. In (3) $\tau_{(1)ij}$ denotes Oldroyd's upper convected derivative of τ_{ij} given by

$$\tau_{(1)ij} = \frac{\partial \tau_{ij}}{\partial t} + u_k \frac{\partial \tau_{ij}}{\partial x_k} - \tau_{kj}\frac{\partial u_i}{\partial x_k} - \tau_{ik}\frac{\partial u_j}{\partial x_k} \tag{4}$$

The mass and momentum conservation equations and the constitutive equation obey the principle of invariance and are written for an orthogonal coordinate system (x_1, x_2, x_3). Their discretization on a general computational finite-volume mesh composed of non-orthogonal six-faced cells requires transformation to a general non-orthogonal coordinate system (ξ_1, ξ_2, ξ_3) and it is advantageous from a numerical point of view (Ferziger and Peric, 1996) to write the equations in a strong conservation form so that the final algebraic equations will retain that property. The transformation rules and other details are presented in Oliveira et al (1997) and the final equations to be numerically solved are

- continuity

$$\frac{\partial}{\partial \xi_l}\left(\rho \beta_{lj} u_j\right) = 0 \tag{5}$$

- momentum

$$\frac{\partial}{\partial t}\left(J\rho u_i\right) + \frac{\partial}{\partial \xi_l}\left(\rho \beta_{lj} u_j u_i\right) - \frac{\partial}{\partial \xi_l}\left(\frac{\eta}{J}\beta_{lj}\beta_{lj}\frac{\partial u_i}{\partial \xi_l}\right) =$$

$$-\beta_{li}\frac{\partial p}{\partial \xi_l} + \frac{\partial}{\partial \xi_l}\left(\beta_{lj}\tau_{ij}\right) + J\rho g_i - \frac{\partial}{\partial \xi_l}\left(\frac{\eta}{J}\beta_{lj}\beta_{lj}\frac{\partial u_i}{\partial \xi_l}\right) \tag{6}$$

- constitutive equation

$$J\tau_{ij} + \lambda\frac{\partial}{\partial t}\left(J\tau_{ij}\right) + \lambda\frac{\partial}{\partial \xi_l}\left(\beta_{lk}u_k\tau_{ij}\right) = \eta\left[\beta_{lj}\frac{\partial u_i}{\partial \xi_l} + \beta_{li}\frac{\partial u_j}{\partial \xi_l}\right] +$$

$$\lambda\left[\left(\beta_{lk}\tau_{kj}\right)\frac{\partial u_i}{\partial \xi l} + \left(\beta_{lk}\tau_{ki}\right)\frac{\partial u_j}{\partial \xi_l}\right] - \frac{2}{3}\eta\beta_{lk}\frac{\partial u_k}{\partial \xi_l}\delta_{ij} \tag{7}$$

3. NUMERICAL METHOD

The numerical method was presented in detail in Oliveira et al (1998) so here only a brief description is given. The calculation domain is subdivided in many non-overlapping cells, and Eqs. (5) to (7) are volume-integrated in each cell with the help of Gauss' theorem so that full conservativeness is insured. The resulting equations are then discretized with some differencing scheme which enables substitution of the derivatives by algebraic expressions in terms of variable values calculated at the centre of the cells and at the centre of their faces.

The discretised mass conservation Eq. (8) is required for the calculation of the pressure and becomes

$$\sum_{f}^{6}(-1)^f F_f = 0 \tag{8}$$

where the $(-1)^f$ is used to yield positive outgoing convective fluxes F_f, calculated as

$$F_f = \sum_j \left(\rho B_{fj}\tilde{u}_j\right)_f \tag{9}$$

with face index f = 1 to 6 for w, e, s, n, b and t, where compass notation is used.

The momentum Eq. (6) can be casted under the common linearised form for the velocity component u_i

$$a_P u_{i-P} = \sum a_f u_{i-f} + S_{u_i} + \frac{\rho V_P}{\delta t}u^o_{i-P} \tag{10-a}$$

where

$$a_P = \frac{\rho V_P}{\delta t} + a_0 + S_P,$$

$$a_o \equiv \sum a_f \tag{10-b}$$

and u^o_{i-P} refers to the velocity at the previous time level and the coefficients of the neighbour cells (a_f, with F spanning the near-neighbouring cells of cell P) have convective (a^C_f) and diffusive (a^D_f) contributions:

$$a^D_f = \frac{\eta_f}{V_f}\left(B_f\right)^2 \tag{11-a}$$

$$a^C_f = \max(F_f, 0) \tag{11-b}$$

The convective contribution in Eq. (11) pertains to the upwind scheme (UDS) and for those of the linear-upwind the reader is referred to Oliveira et al (1998).

The total source term S_{ui} of the momentum equation has contributions from all the terms on the right-hand-side of Eq. (6) and is given by:

$$S_{u_i} = S_{ui-pressure} + S_{ui-gravity} + S_{ui-stress} + S^D_{ui} + \sum a_{ff} u_{i-ff} \tag{12}$$

where the various terms on the rhs represent the pressure gradient, gravity, stress field divergence and the added diffusion terms, respectively.

The last term on the rhs of Eq. (12) involves far-neighbour points which originate from the use of a second-order accurate linear upwind scheme (LUDS) as the interpolation scheme for the convective terms.

The discretized stress equation has a similar outlook to the momentum Eq. (10-a)

$$a^\tau_P \tau_{ij-P} = \sum_f a^\tau_f \tau_{ij-f} + S_{\tau_{ij}} + \frac{V_P}{\delta t}\tau^0_{ij-P} \tag{13}$$

except for the absence of diffusive terms in the stress coefficients a_f. These coefficients are identical to those in the momentum equation except that they need to be multiplied by λ/ρ, i.e., any

$$a_f \text{ for stress} = \frac{\lambda}{\rho} a_f^C \text{ for momentum} \qquad (14)$$

All the other contributions to the constitutive equation go to the source. The central coefficient of cell P is computed from Eq. (15) below with near- and far-neighbour points in the summation due to the higher order scheme LUDS.

$$a_P = V_P + \frac{\lambda V_P}{\delta t} + \sum_{f+ff} a_f^T \qquad (15)$$

Convective terms of the momentum and stress equations involve first derivatives of the quantities being convected, and thus lead to values of those quantities at the faces of the cells. These face values need to be computed from nodal values, a procedure which is based on an interpolation scheme. In this work the second order accurate linear upwind scheme, explained in Ferziger and Peric (1996), was used and the reader is also referred to Pinto (1996) for the equations for the convective coefficients.

The handling of the convective fluxes adopted here is based on the special interpolation scheme of Rhie and Chow (1982), with some modifications designed to avoid the problem of the final solution being dependent on the particular time-step used in the calculations, as explained in Issa and Oliveira (1994). Similarly a special interpolation technique developed by Oliveira et al (1998) is applied to evaluate all cell face stresses required in the divergence of the stress tensor terms in the momentum equation

$$S_{u_{i-stress}} = \sum_f \sum_j B_{fi} \tilde{\tau}_{ij,f} \qquad (16)$$

in Eq. (12).

The solution algorithm is a modified version of the SIMPLEC algorithm of Van Doormal and Raithby (1984) extended to account for the stress equations. This algorithm was originally developed for iterative time-marching, but here we adopt instead the time-marching version explained in Issa and Oliveira (1994).

The presence of a complex constitutive equation produces little changes upon the original SIMPLEC method, which is only concerned with the calculation of the pressure. Two new steps are introduced in the SIMPLE-like algorithm to account for the stress equations and they are:

- The calculation of the stress tensor from the six implicit constitutive equations, which must be carried out before solving the three momentum equations. The coefficients and source term are based on previous time-level velocity and stress values.
- Then, the momentum equations are solved implicitly for each velocity component with the stress obtained above going to the source term. The important step here is to evaluate the divergence term (16) with cell-face stresses based on the specially developed interpolation practice of Oliveira et al (1998). The velocities at this stage do not satisfy the continuity equation and the algorithm proceeds as in the classical SIMPLEC case with further corrections of the velocity and pressure in order to satisfy momentum and mass continuity.

Boundary conditions are required for the dependent quantities at the boundary faces of the computational domain. At inlet, fully developed flow conditions were imposed.

The outlet was far away downstream of the region of interest, where profiles become approximately fully developed, so zero streamwise gradients can be safely assumed for the velocity stress and pressure gradients.

For the symmetry planes fictitous cells may be created in which reflexion laws apply according to Oliveira et al (1998) and in this way only half the domain is required.

For solid walls the no-slip condition applies to all velocity components. The pressure is linearly extrapolated from the two nearest neighbour cells, a practice used in classical Newtonian CFD (Ferziger and Peric, 1996). The stress components are given implicitly by an equation derived from the constitutive equation after equating to zero the convective terms. This equation is incorporated into the general iterative procedure and solved sequentially to yield the stress value at the wall art he last iteration.

FLOW GEOMETRY AND COMPUTATIONAL MESH

Fig. 1 defines the coordinate system, nomenclature and indicates the structured blocks used to generate the computational meshes in the sudden contraction of the UCM fluid, the same problem considered by Sato and Richardson (1994). In the longitudinal direction the calculation domain for the base case spans from -10 to +10 downstream channel half-heights, H_2. The upstream length was sufficient for the inlet fully developed profile to be maintained for some distance before the contraction, whereas the downstream length was sufficient for the flow at the contraction plane to be unaffected by the outlet conditions and for the flow to become locally parabolic near the exit. Both conditions were preliminary verified with longer calculation domains. The Reynolds and Deborah numbers are defined on the basis of the dowsntream channel quantities as

$$\mathrm{Re} = \frac{\rho U_2 H_2}{\eta}$$

$$De = \frac{\lambda U_2}{H_2}$$

and could be varied independently by changing appropriate the model parameters.

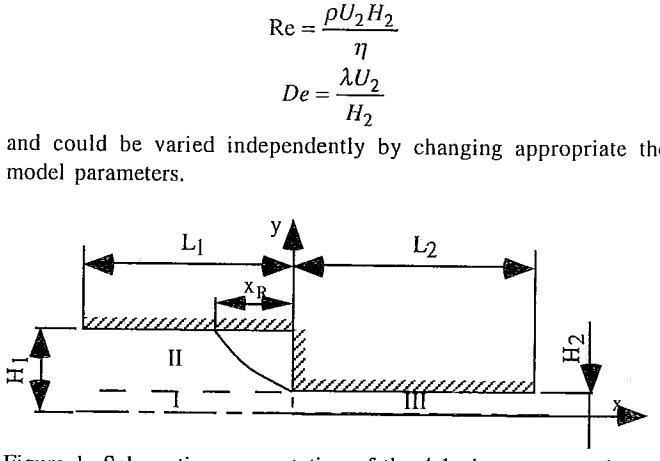

Figure 1- Schematic representation of the 4:1 planar contraction.

These definitions are in agreement with those in the literature, namely the works of Purnode and Crochet (1996), Evans and Walters (1986), Baloch et al (1995) and Sato and Richardson (1994).

The results in this paper pertain to the UCM fluid and were obtained for a Reynolds number of 0.01 (representative of creeping flow) and Deborah numbers from 0 to 10, clearly in excess of the

Table I- Main mesh characteristics

	Block I			Block II			Block III		
	NX x NY	f_x	f_y	NX x NY	f_x	f_y	NX x NY	f_x	f_y
mesh1	40 x 20		0.95	40 x 40		1.0436	40 x 20		0.95
mesh2	60 x 20	0.95367	0.95	60 x 40	0.95367	1.0436	60 x 20	1.04858	0.95
mesh4	80 x 40	0.9519	0.9595	80 x 67	0.9519	*1.0486 + 0.9270	80 x 40	1.0505	0.9595

* this block was actually divided into two blocks so that the cells could also be concentrated on the inlet channel wall and to resolve well the salient corner

maximum values obtained by Yoo and Na (1991), Marchal and Crochet (1987) and more recently Xue et al (1998), with the added consideration that here the meshes were much finer. With regard to the differencing schemes converged solutions were obtained with UDS up to De= 10 and LUDS was used for some of the lower De cases (0 to 3).

The two-dimensional geometry was divided into three blocks for the purpose of generating the computational meshes, as in Fig. 1, with blocks I and II in the inlet channel and block III in the outlet channel.The cells were made smaller as the contraction plane and the re-entrant corner were approached, using appropriate geometrical factors, so that at the corner the minimum normalised cell size was $\delta_{x\,\min}/H_2 = \delta_{y\,\min}/H_2 = 0.01$ for the finest mesh 4 and 0.03 and 0.05 for the two coarser meshes 2 and 1, respectively. The main characteristics of the computational meshes are summarised in Table I. Mesh 3, not listed in Table I, had characteristics similar to mesh 1 but with a longer inlet length ($L_1 = 20H_2$) was used to assess the effects of varying L_1.

All the results to be presented were computed with the finest mesh unless otherwise stated.

RESULTS AND DISCUSSION

Since the interest from the outset was to verify whether the flow patterns of a UCM fluid in a planar contraction change as the fluid elasticity is increased, specifically to verify whether lip vortices and vortex enhancement are present for the 4:1 contraction ratio, we start by presenting the predicted streamlines for increasing Deborah number. Fig. 2 thus shows the resulting streamlines for a UCM fluid for Deborah numbers ranging from 0 to 8, as obtained in the fine mesh 4. These streamlines were based on calculations where the UDS discretization scheme was used for representing the first derivative after assessing its effects upon the predictions (to be shown later). The results in Fig. 2 show an increase of both the size and the intensity of the salient corner vortex with fluid elasticity. Vortex size is here measured by its non-dimensional length ($X_R = x_R/H_2$) and intensity is measured by the maximum amount of recirculating flow relative to the inlet flow rate (thus, intensity $\Psi_R = \Psi_{max} - 1$). The figure also shows that at $De \approx$ 1.0-1.5 a small lip vortex is formed at the re-entrant corner. As the Deborah number is increased the salient corner vortex tends to finger towards the re-entrant corner, and the two vortices merge at about De= 2. At De= 2 and De= 3 the two vortices are clearly outlined in the streamline plots, whereas at De= 6 the merging process is complete and there is now a single strong salient-corner recirculating region. Note that at lower Deborah numbers the boundary of the bubble has a typical straight or concave shape, which becomes more concave when the two vortices are present, but then changes into a convex shape once the corner and lip vortices merge into a single recirculating region. This is in agreement with observations reported in the literature (Yoo and Na (1991), Purnode and Crochet (1996) and Xue et al (1998)) for a similar situation but with the Oldroyd-B and FENE-P models. Another feature seen in Fig. 2 is that the size of the vortex is approximately constant in the range of the Deborah numbers during which the lip and corner vortices co-exist and only starts increasing with De after the merging process is complete. For the Newtonian flow case, the recirculation length normalised with the upstream channnel width ($x_R/2H_1$) is equal to 0.172, in agreement with results reported by Sato and Richardson (1994), and is increased to 0.283 at De= 8.

In our view the inability of previous work to predict the lip vortex mechanism in the planar contraction with the the UCM fluid did stem from one main reason: insufficient mesh refinement leading to inaccurate results. The effect of Reynolds number is important to establish the size and strength of the vortex pattern, as already noticed by Yoo and Na (1991). However we did not find it to be the decisive factor in the appearance of the lip vortex; our results for creeping flow (Re=0) and for Re= 0.01 were virtually identical, both exhibiting lip vortex at De= 2 (c.f. Fig. 2-d). Xue et al (1998) came to the same conclusion in their recent work.

Importance of mesh refinement is well exemplified by Fig. 3, where the variation of the normalised vortex intensity (Ψ_R) and size (X_R) are shown as a function of the Deborah number for different meshes and differencing schemes. The coarse mesh (mesh 1) is seen to give rise to erroneous longer and stronger recirculation zones, especially at Deborah numbers in excess of 2 or 3, in the range where there is already a single increasing corner vortex. In the low Deborah number region (for De < 2) the lip vortex is formed, the corner vortex fingers towards the lip and the two vortices finally merge and discrepancies between the results of the two meshes are enhanced, especially in the magnitude of the maximum recirculating flow rate. In the Deborah number range for which a lip vortex is predicted with the finer mesh, Ψ_R turns out to be approximately constant because increased elasticity tends to enhance the lip vortex intensity at the expense of the corner vortex. It is stressed that the Ψ_R in the figure is not the total recirculating flow in the vortices unless there is a single vortex present. The size of the recirculation is also approximately constant in that Deborah number range. Fig. 3 also shows that the higher order scheme (LUDS-closed marks in the Fig.) tends to bring the predictions with the medium mesh more in agreement with those of the fine mesh, thus indicating the benefits of adopting a higher order scheme, especially for the hyperbolic constitutive equation.

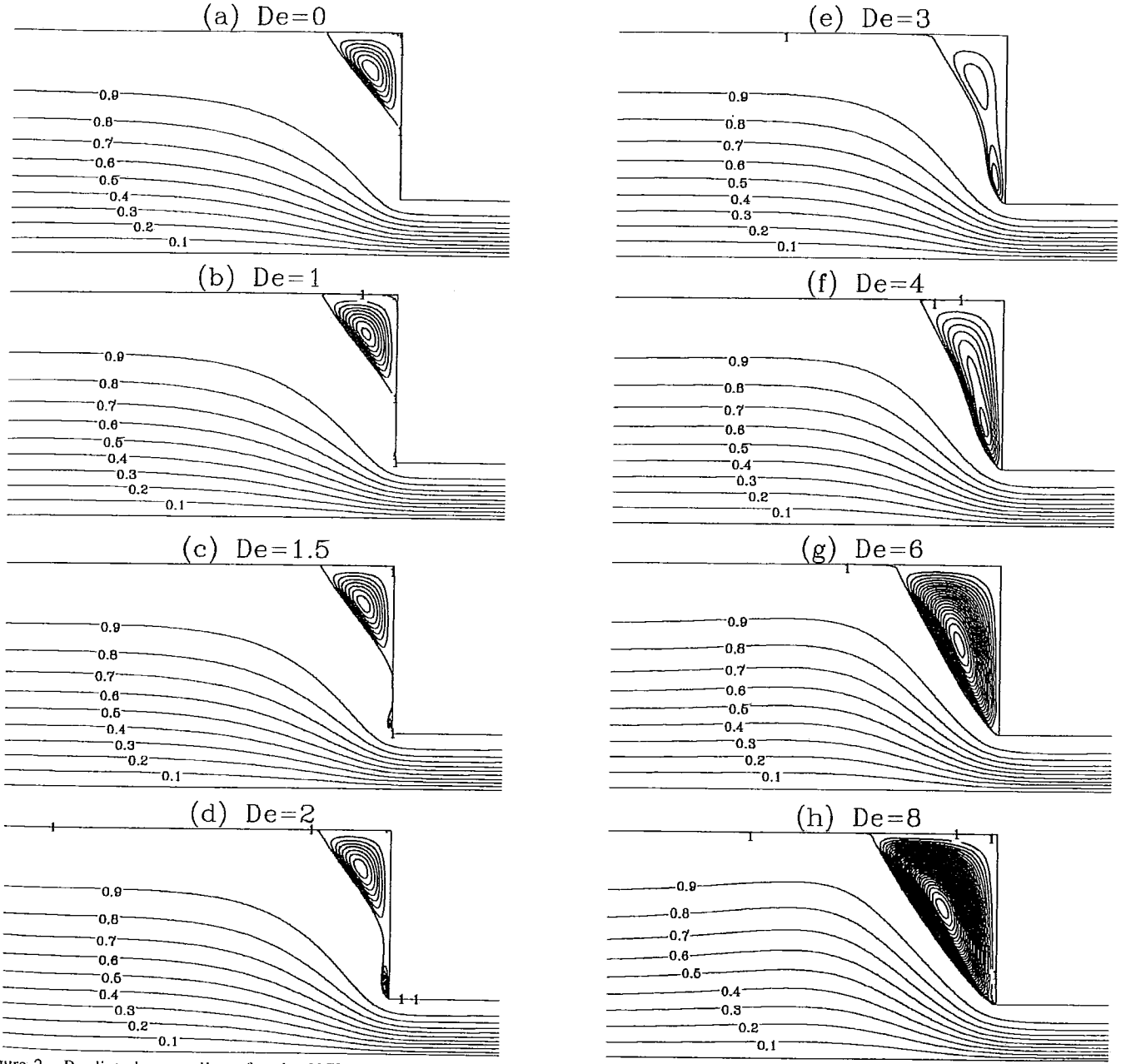

Figure 2- Predicted streamlines for the UCM fluid at Re= 0.01 in the fine mesh with the UDS scheme. Streamlines in the recirculation are equally spaced: with $\delta_\psi = 10^{-4}$ for De≤ 2 and $\delta_\psi = 5\times10^{-4}$ for De > 2.

The effect of mesh refinement upon local variables is also observed in Fig. 4-a) where the fine mesh leads to higher and sharper normal stress profiles along the line y= 0.985, passing nearby the geometric singularity. It is not so evident in the velocity profiles of Fig. 4-b), except in the coarser mesh where some oscillations, due to bad resolution coupled with high gradients, are seen near the re-entrant corner. Accuracy is also affected by the level of elasticity. Fig. 4-c) shows the predicted normal stress variations along the centreline for various Deborah numbers in the coarse and fine meshes. If the stress scale was the same as in Fig. 4-a) presumably no discernable differences between the predictions in the two meshes would be observed. Even with the enlarged scale of Fig. 4-c) it is quite clear that the normal stress difference along the contraction centreline is much less sensible to mesh refinement and one essentially finds mesh-independent results for *De*= 2. However, the important point here is that if the fluid elasticity is increased from *De* of 2 to 8, then mesh 1 is clearly inadequate to resolve the N_1 evolution along the centreline. Hence, in numerical predictions of highly elastic fluids, the computational

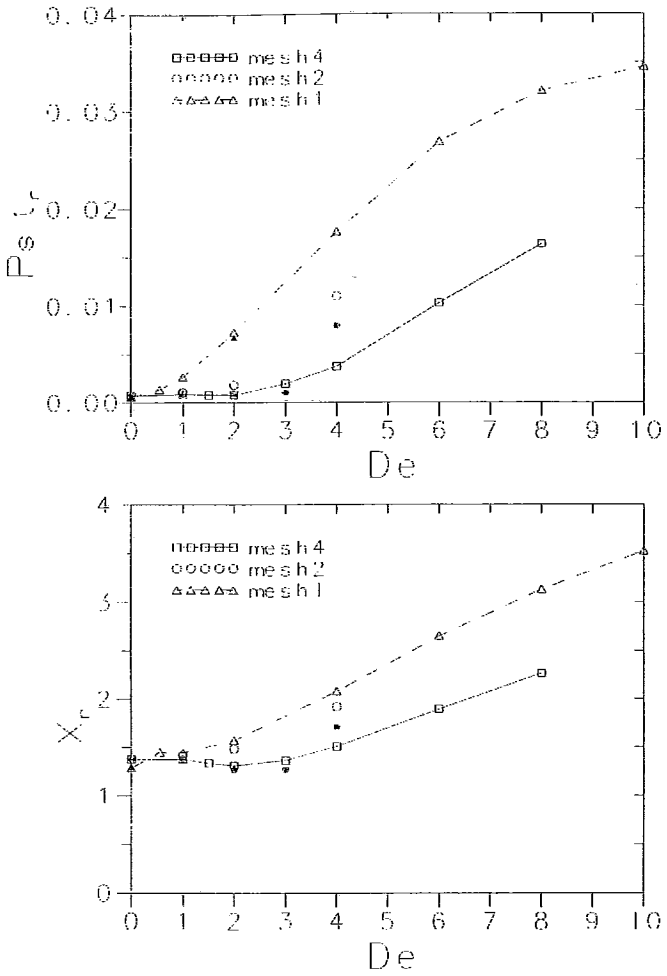

Figure 3- Effect of mesh refinement on the maximum normalised stream function ($\Psi_R = \Psi_{max} - 1$) and normalised recirculation length (x_R/H_2) as a function of the Deborah number at Re= 0.01. (Open symbols, UDS; Closed symbols, LUDS).

meshes have to be finer than those which were adequate for less elastic fluids.

The computational meshes used in the present work are much finer than those used by Marchal and Crochet, even considering that their finite elements possess additional internal points and, in fact, their results agree well with our predictions when these are produced with our coarser mesh. However, it is already apparent that the coarse mesh results are too inaccurate (c.f. Fig. 3). The effect of mesh refinement on the flow pattern can be assessed from Fig. 5, which refers to a Deborah number of 2. In the finer mesh, separation between the lip and corner vortices is clearly seen and is still present in the medium sized mesh, though here interaction between the two vortices increased and the lip vortex is larger. In the coarser mesh, however, the re-entrant corner vortex has grown so much towards the salient corner vortex that both have merged into a single vortex. All these differences in flow patterns are

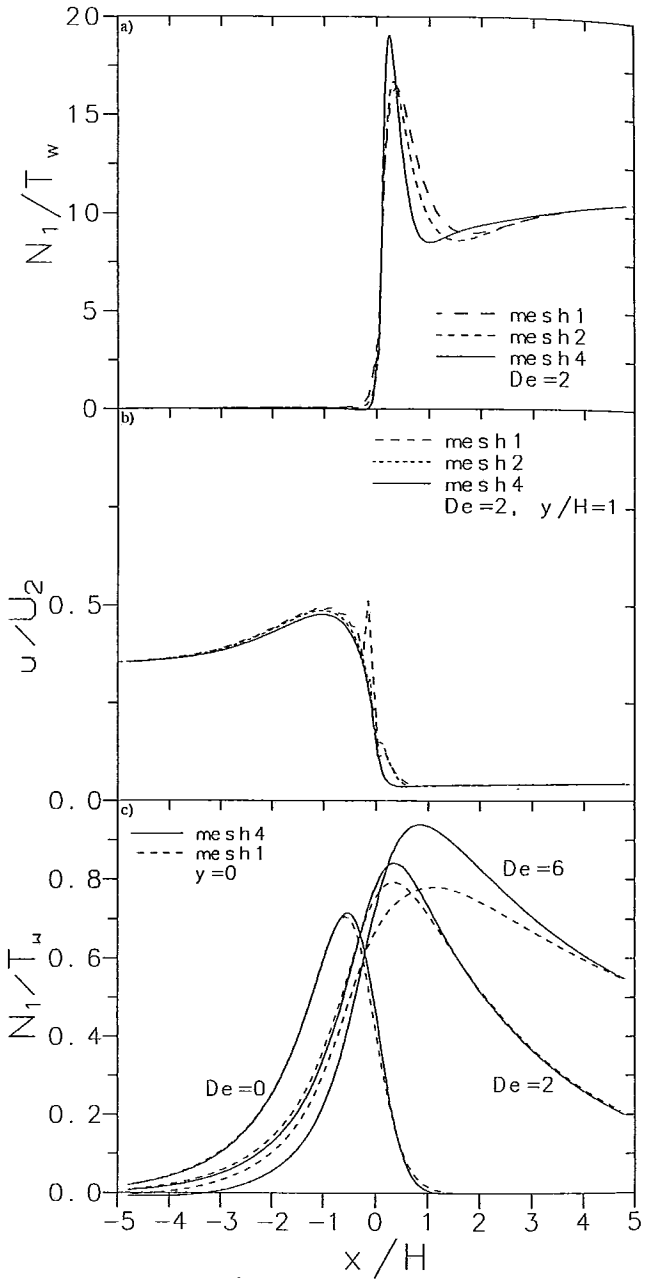

Figure 4- Effect of mesh refinement on the longitudinal profiles of (a) N_1/T_w at $y/H_2 = 0.985$; (b) u/U_2 at $y/H_2 = 0.985$; (c) N_1/T_w at $y/H_2 = 0$.

purely a consequence of the refinement of the mesh used; the flow field which is a solution to the differential equations is obviously unique and is expected to be closer to that shown in Fig. 5-a). The issue of mesh refinement has also been addressed by Xue et al (1998) and the deterioration in the predictions of flow pattern observed here with coarser meshes, near the contraction plane, is very similar to the results of their Fig. 5-b). Note, however, that in the present work the smallest mesh spacing was still 40% finer and that the number of cells were in excess of 100% and still we are able

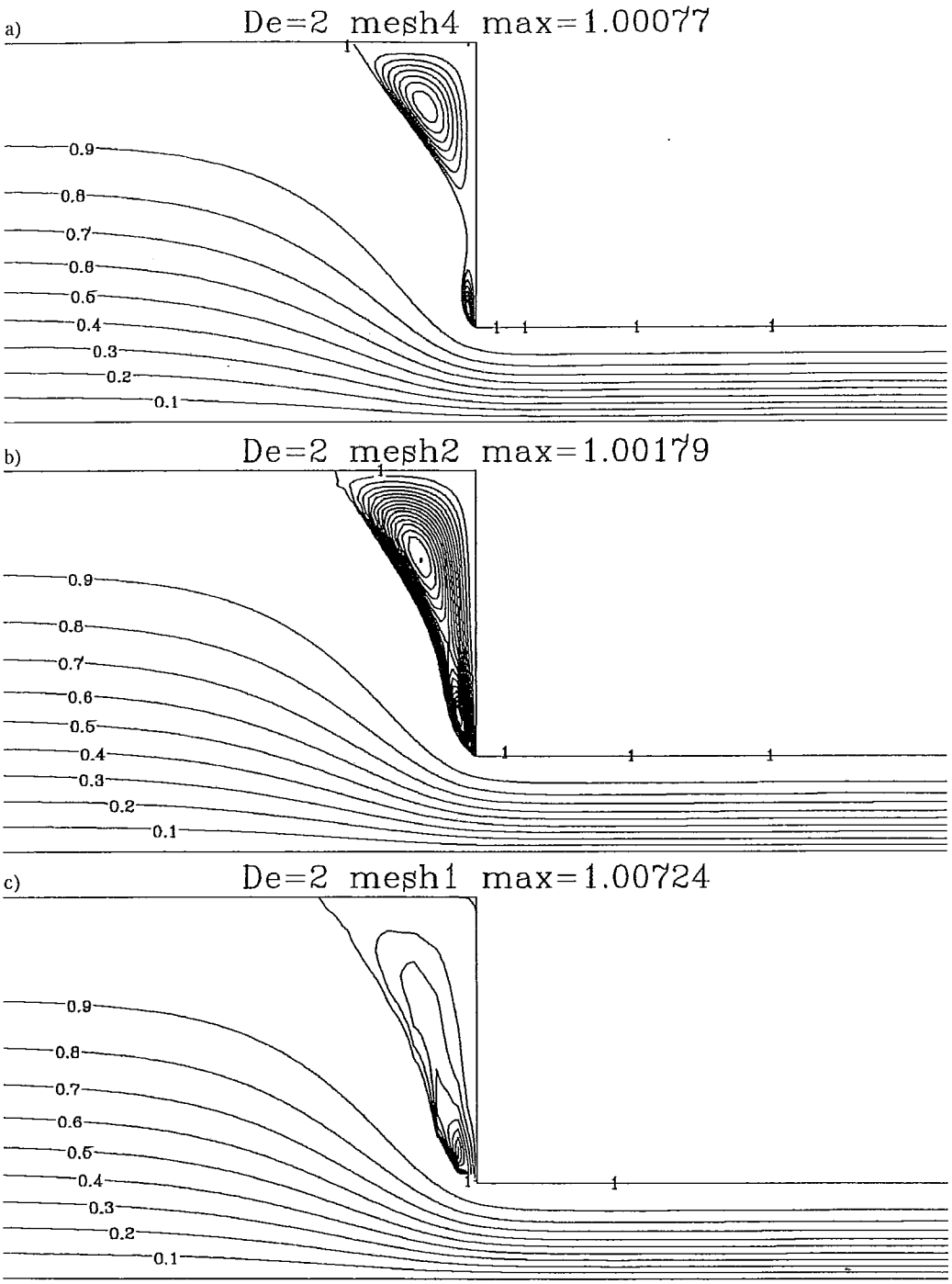

Figure 5- Effect of mesh refinement on the flow pattern of the UCM fluid at De= 2. (a) fine mesh $\left(\delta_\Psi = 10^{-4}\right)$; (b) medium mesh $\left(\delta_\Psi = 10^{-4}\right)$; (c) coarse mesh $\left(\delta_\Psi = 10^{-3}\right)$; ($\delta_\Psi \equiv$ streamline spacing in the recirculation; maximum streamline values are indicated).

to report a lip vortex with the UCM model which bears some resemblance to what they predicted with an Oldroyd-B fluid. This resulted from the significant proportion (45.5%) of the 8379 cells used by Xue et al (1998), to represent the contraction geometry, that had to be blocked to account for the walls.

It is well known that the use of a first order upwinding scheme to represent the convective terms may introduce numerical diffusion and this has been felt in this work. It is emphasised that for the Reynolds numbers from 0.01 up to unity the problem is

confined to the convective terms in the constitutive equations and is absent

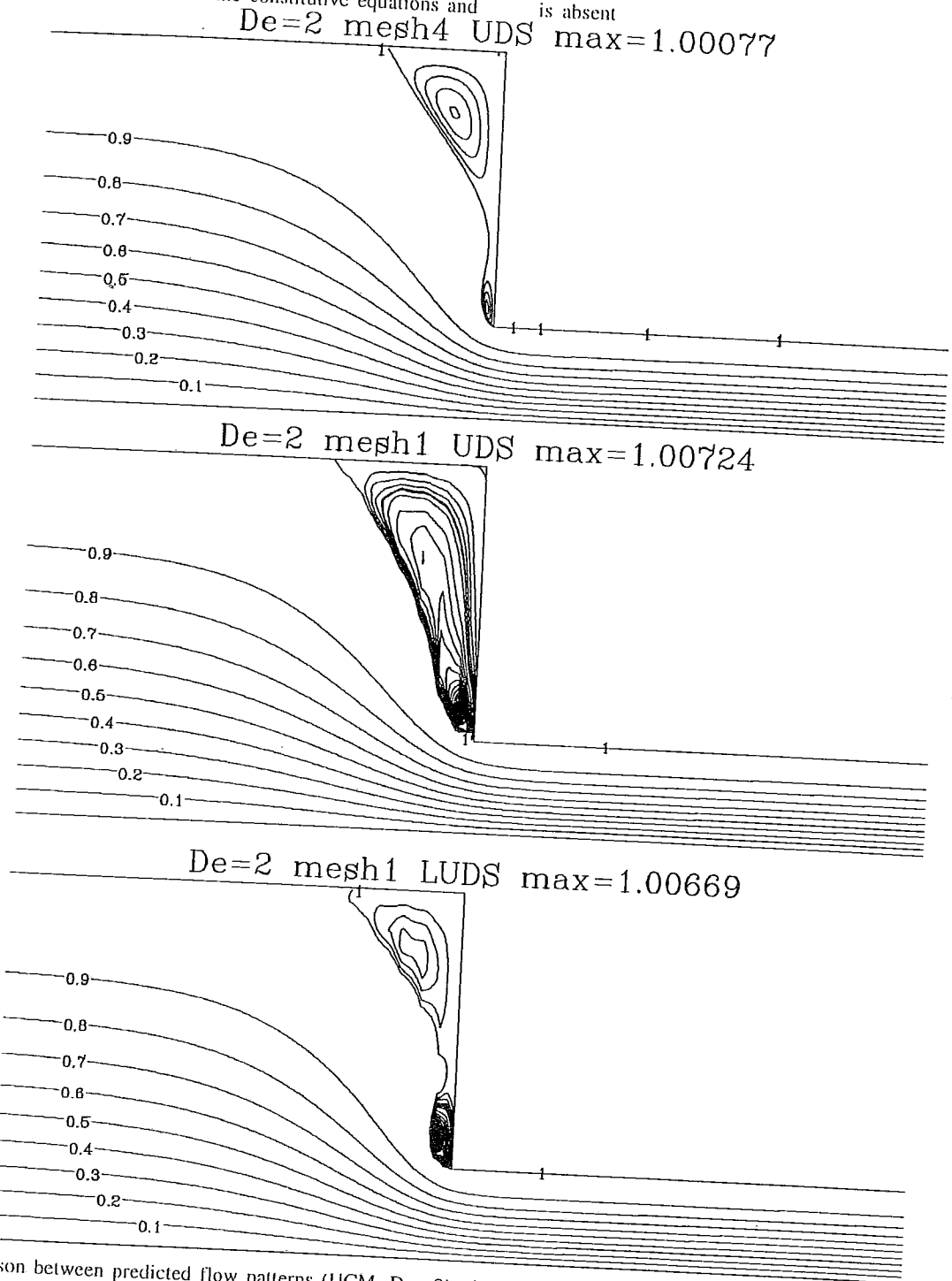

Figure 6- Comparison between predicted flow patterns (UCM, De= 2): (i) in the fine mesh; (ii) in the medium mesh with UDS; (iii) in the medium mesh with LUDS.

from the convective terms in the momentum equations. In fact it has been checked that the results are virtually identical for Newtonian fluids (De= 0), using either UDS or LUDS. Fig. 6 compares streamlines obtained with the medium sized grid using UDS and the second order accurate linear upwind scheme, LUDS.

The finer mesh calculation with UDS is also included and all the runs pertain to a Deborah number of 2 and a Reynolds number of 0.01. The lip vortex is present in the re-entrant corner, as we can see in the finer mesh plot, but artificially grows as the mesh becomes coarser and the less accurate differencing scheme is

utilised, but is reduced to the "right" size with the higher order scheme. In this particular instance the use of LUDS instead of UDS affects both the salient corner vortex, whose intensity and size are properly predicted with LUDS becoming very similar to the fine mesh results, and the lip vortex whose size and shape is also better predicted with LUDS. Note, however, that convergence is more difficult to attain with the LUDS scheme and thus it was found easier to obtain converged solutions using a finer grid together with the UDS scheme.

Hence, it can be concluded that the streamline pattern of a UCM fluid flowing in a 4:1 planar contraction is rather more complex than reported in previous numerical work (c.f. Marchal and Crochet, 1987), sharing the usual characteristics seen in experiments, but these features can only be predicted if very fine meshes are used in the computations. Another specific difference between the present work and that of Marchal and Crochet (1987) lies on the numerical method: they used a finite-element method whereas here it is a finite-volume method, requiring far less memory and CPU, but allowing for the same generality as their finite-element method.

CONCLUSIONS

A general finite-volume method based on an efficient collocated mesh arrangement for non-ortogonal geometries, with the added advantage of indirect addressing, has been applied to the prediction of the flow of UCM fluids in the 4:1 planar sudden contraction geometry. Both first and second order discretization schemes for convection were used and the Deborah number varied from 0 to 10 at a constant Reynolds number of 0.01. No special artifacts, such as extra diffusion in the stress equation, were necessary to obtain converged solutions with the finer computational meshes utilised.

The predicted flow patterns showed all the complex features seen in flow visualisation and also in recent numerical simulations of contraction flows: corner Moffat vortex, lip vortex, fingering and merging of the two vortex types, and single vortex growth with increasing Deborah number.

The results show the growth of the salient corner vortex with fluid elasticity and the presence of a lip vortex at Deborah numbers of about 2. Fingering from the corner vortex towards the re-entrant corner is also observed. These features require the use of very fine meshes and are in contrast with some earlier investigations reported in the literature (e.g. Marchal and Crochet (1987) and Song and Yoo, 1987), who investigated the same flow but used finite-element or finite-difference methods in coarser meshes. It is however noted that in a few studies with the Oldroyd-B model the presence of lip vortices has been reported, although in some instances these vortices have not been well resolved at all, as in Yoo and Na (1991), and in others they were attributed to transient effects, as in Sato and Richardson (1994).

ACKNOWLEDGEMENTS

The authors acknowledge the financial support of project PBIC/P/QUI/1980/95 of JNICT without which this work could not have been carried out.

REFERENCES

Baloch, A, Townsend, P. and Webster, M. F. 1995 "On the simulation of highly elastic complex flows" J. Non-Newt. Fluid Mech., vol. 59, 111.

Boger, D. V., and Hur, D. U. and Binnington, R. J. 1986. "Further observations of elastic effects in tubular entry flows" J. Non-Newt. Fluid Mech., vol. 20, 31.

Boger, D. V. 1987. "Viscoelastic flows through contractions" Ann. Rev. Fluid Mech., vol. 19, 157.

Evans, R. E. and Walters, K. 1986. "Flow characteristics associated with abrupt changes in geometry in the case of highly elastic liquids" J. Non-Newt. Fluid Mech., vol. 20, 11.

Ferziger, J. H. and Peric, M. 1996 "Computational Methods for Fluid Dynamics." Springer Verlag, Berlin

Issa, R. I. and Oliveira, P. J. 1994. "Numerical predictions of phase separation in two-phase flow through T-junctions." Computers and Fluids, vol. 23, 347-372.

Oliveira, P. J., Pinho, F. T. and Pinto, G. A. 1997. "A finite-volume collocated-mesh method for the prediction of non-Newtonian fluid flow" FED Vol. 243 , MD Vol. 78: Rheology and Fluid Mechanics of Non-Linear Materials of ASME 1997 International Mechanical Engineering Congress and Exposition, Dallas, November 1997, 119-131.

Oliveira, P. J., Pinho, F. T. and Pinto, G. A. 1998. "Numerical simulation of non-linear elastic flows with a general collocated finte-volume method" J. Non-Newt. Fluid Mech., vol. 79, 1.

Marchal, J. M. and Crochet, M. F. 1987. "A new mixed finite element for calculating viscoelastic flow" J. Non-Newt. Fluid Mech., vol. 26, 77.

Pinto, G. A. 1996. "Development of a Numerical Simulation Programme for the Calculation of Laminar Flows with Non-Linear Elastic Fluids" (in portuguese). MSc. Thesis, University of Porto, Portugal.

Purnode, B. and Crochet, M. 1996 "Flows of polymer solutions through contractions. Part 1: flows of polyacrylamide solutions through planar contractions" J. Non-Newt. Fluid Mech., vol. 65, 269.

Rhie, C. M. and Chow, W. L. 1982. "A numerical study of the turbulent flow past an isolated airfoil with trailing edge separation." AIAA, vol. 82, 998.

Sato, T. and Richardson, S 1994. "Explicit numerical simulation of time-dependent viscoelastic flow problems by a finite element/finite volume method" J. Non-Newt. Fluid Mech., vol. 51, 249.

Song, S. H. and Yoo, J. Y. 1987. "Numerical simulation of viscoelastic flow through a sudden contraction using a type dependent difference method" J. Non-Newt. Fluid Mech., vol. 24, 221.

Van Doormal, J. P.and Raithby, G. D. 1984. "Enhancements of the SIMPLE method for predicting incompressible fluid flows." Num. Heat Transfer, vol. 7, 147-163.

Xue, S.- C., Phan-Thien, N. and Tanner, R. I. 1998 "Three dimensional numerical simulations of viscoelastic flows through planar contractions" J. Non-Newt. Fluid Mech., vol. 74, 195.

Yoo, J. Y. and Na, Y. 1991. "A Numerical Study of the Planar Contraction Flow of Viscoelastic Fluids Using the SIMPLER Algorithm." J. Non-Newt. Fluid Mech., vol. 39, 89-106.

confined to the convective terms in the constitutive equations and is absent

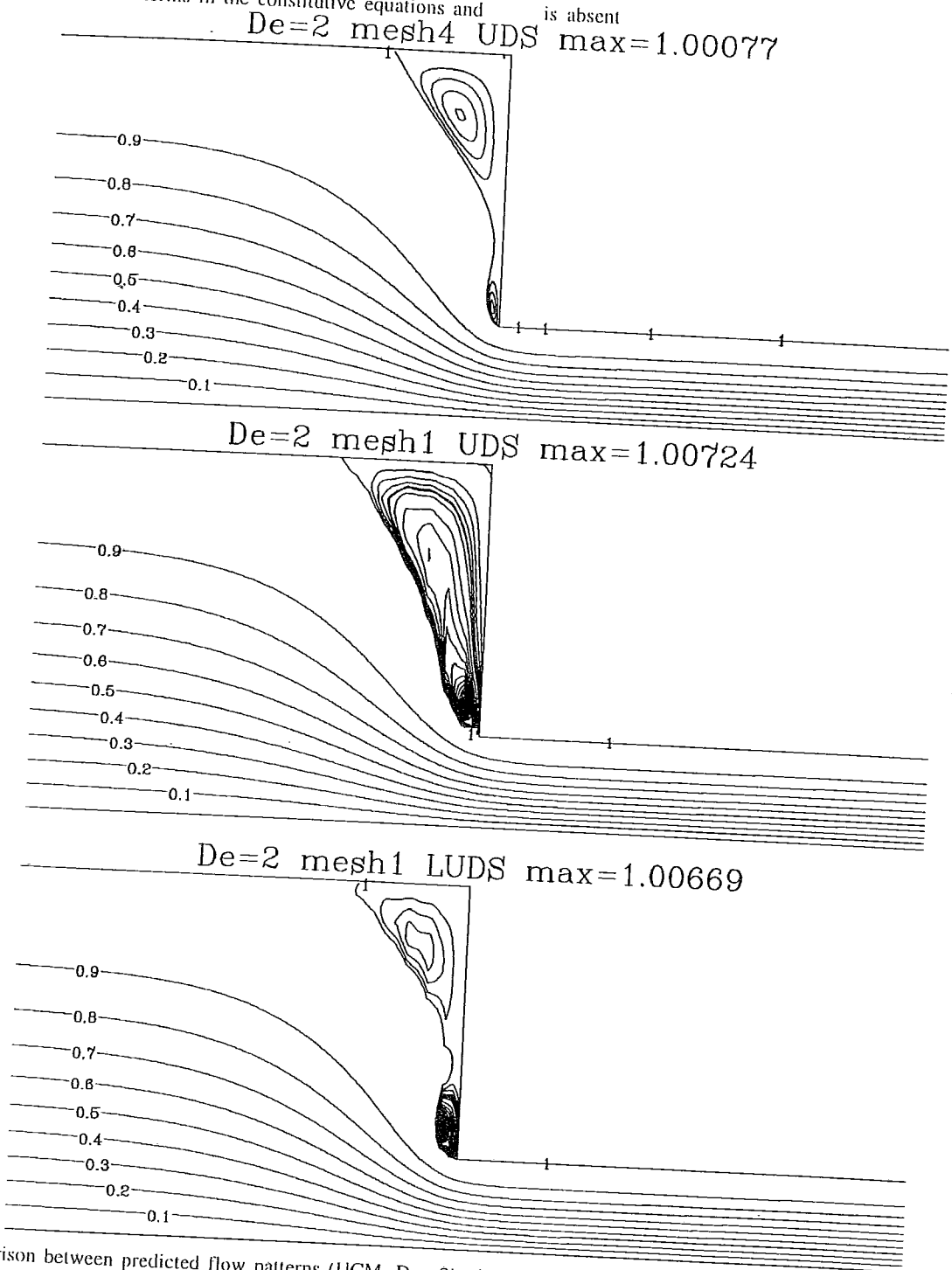

Figure 6- Comparison between predicted flow patterns (UCM, De= 2): (i) in the fine mesh; (ii) in the medium mesh with UDS; (iii) in the medium mesh with LUDS.

from the convective terms in the momentum equations. In fact it has been checked that the results are virtually identical for Newtonian fluids (De= 0), using either UDS or LUDS. Fig. 6 compares streamlines obtained with the medium sized grid using UDS and the second order accurate linear upwind scheme, LUDS.

The finer mesh calculation with UDS is also included and all the runs pertain to a Deborah number of 2 and a Reynolds number of 0.01. The lip vortex is present in the re-entrant corner, as we can see in the finer mesh plot, but artificially grows as the mesh becomes coarser and the less accurate differencing scheme is

utilised, but is reduced to the "right" size with the higher order scheme. In this particular instance the use of LUDS instead of UDS affects both the salient corner vortex, whose intensity and size are properly predicted with LUDS becoming very similar to the fine mesh results, and the lip vortex whose size and shape is also better predicted with LUDS. Note, however, that convergence is more difficult to attain with the LUDS scheme and thus it was found easier to obtain converged solutions using a finer grid together with the UDS scheme.

Hence, it can be concluded that the streamline pattern of a UCM fluid flowing in a 4:1 planar contraction is rather more complex than reported in previous numerical work (c.f. Marchal and Crochet, 1987), sharing the usual characteristics seen in experiments, but these features can only be predicted if very fine meshes are used in the computations. Another specific difference between the present work and that of Marchal and Crochet (1987) lies on the numerical method: they used a finite-element method whereas here it is a finite-volume method, requiring far less memory and CPU, but allowing for the same generality as their finite-element method.

CONCLUSIONS

A general finite-volume method based on an efficient collocated mesh arrangement for non-ortogonal geometries, with the added advantage of indirect addressing, has been applied to the prediction of the flow of UCM fluids in the 4:1 planar sudden contraction geometry. Both first and second order discretization schemes for convection were used and the Deborah number varied from 0 to 10 at a constant Reynolds number of 0.01. No special artifacts, such as extra diffusion in the stress equation, were necessary to obtain converged solutions with the finer computational meshes utilised.

The predicted flow patterns showed all the complex features seen in flow visualisation and also in recent numerical simulations of contraction flows: corner Moffat vortex, lip vortex, fingering and merging of the two vortex types, and single vortex growth with increasing Deborah number.

The results show the growth of the salient corner vortex with fluid elasticity and the presence of a lip vortex at Deborah numbers of about 2. Fingering from the corner vortex towards the re-entrant corner is also observed. These features require the use of very fine meshes and are in contrast with some earlier investigations reported in the literature (e.g. Marchal and Crochet (1987) and Song and Yoo, 1987), who investigated the same flow but used finite-element or finite-difference methods in coarser meshes. It is however noted that in a few studies with the Oldroyd-B model the presence of lip vortices has been reported, although in some instances these vortices have not been well resolved at all, as in Yoo and Na (1991), and in others they were attributed to transient effects, as in Sato and Richardson (1994).

ACKNOWLEDGEMENTS

The authors acknowledge the financial support of project PBIC/P/QUI/1980/95 of JNICT without which this work could not have been carried out.

REFERENCES

Baloch, A, Townsend, P. and Webster, M. F. 1995 "On the simulation of highly elastic complex flows" J. Non-Newt. Fluid Mech., vol. 59, 111.

Boger, D. V., and Hur, D. U. and Binnington, R. J. 1986. "Further observations of elastic effects in tubular entry flows" J. Non-Newt. Fluid Mech., vol. 20, 31.

Boger, D. V. 1987. "Viscoelastic flows through contractions" Ann. Rev. Fluid Mech., vol. 19, 157.

Evans, R. E. and Walters, K. 1986. "Flow characteristics associated with abrupt changes in geometry in the case of highly elastic liquids" J. Non-Newt. Fluid Mech., vol. 20, 11.

Ferziger, J. H. and Peric, M. 1996 "Computational Methods for Fluid Dynamics." Springer Verlag, Berlin

Issa, R. I. and Oliveira, P. J. 1994. "Numerical predictions of phase separation in two-phase flow through T-junctions." Computers and Fluids, vol. 23, 347-372.

Oliveira, P. J., Pinho, F. T. and Pinto, G. A. 1997. "A finite-volume collocated-mesh method for the prediction of non-Newtonian fluid flow" FED Vol. 243 , MD Vol. 78: Rheology and Fluid Mechanics of Non-Linear Materials of ASME 1997 International Mechanical Engineering Congress and Exposition, Dallas, November 1997, 119-131.

Oliveira, P. J., Pinho, F. T. and Pinto, G. A. 1998. "Numerical simulation of non-linear elastic flows with a general collocated finte-volume method" J. Non-Newt. Fluid Mech., vol. 79, 1.

Marchal, J. M. and Crochet, M. F. 1987. "A new mixed finite element for calculating viscoelastic flow" J. Non-Newt. Fluid Mech., vol. 26, 77.

Pinto, G. A. 1996. "Development of a Numerical Simulation Programme for the Calculation of Laminar Flows with Non-Linear Elastic Fluids" (in portuguese). MSc. Thesis, University of Porto, Portugal.

Purnode, B. and Crochet, M. 1996 "Flows of polymer solutions through contractions. Part 1: flows of polyacrylamide solutions through planar contractions" J. Non-Newt. Fluid Mech., vol. 65, 269.

Rhie, C. M. and Chow, W. L. 1982. "A numerical study of the turbulent flow past an isolated airfoil with trailing edge separation." AIAA, vol. 82, 998.

Sato, T. and Richardson, S 1994. "Explicit numerical simulation of time-dependent viscoelastic flow problems by a finite element/finite volume method" J. Non-Newt. Fluid Mech., vol. 51, 249.

Song, S. H. and Yoo, J. Y. 1987. "Numerical simulation of viscoelastic flow through a sudden contraction using a type dependent difference method" J. Non-Newt. Fluid Mech., vol. 24, 221.

Van Doormal, J. P.and Raithby, G. D. 1984. "Enhancements of the SIMPLE method for predicting incompressible fluid flows." Num. Heat Transfer, vol. 7, 147-163.

Xue, S.- C., Phan-Thien, N. and Tanner, R. I. 1998 "Three dimensional numerical simulations of viscoelastic flows through planar contractions" J. Non-Newt. Fluid Mech., vol. 74, 195.

Yoo, J. Y. and Na, Y. 1991. "A Numerical Study of the Planar Contraction Flow of Viscoelastic Fluids Using the SIMPLER Algorithm." J. Non-Newt. Fluid Mech., vol. 39, 89-106.